Redox-active compound generated by bacterial crosstalk induces hypha branching in *Streptomyces* species

Manami Kato, [a] Shumpei Asamizu, [a,b]# Hiroyasu Onaka [a,b]#

[a] Graduate School of Agricultural and Life Sciences, The University of Tokyo, Bunkyo, Tokyo, Japan

[b] Collaborative Research Institute for Innovative Microbiology (CRIIM), The University of Tokyo, Bunkyo, Tokyo, Japan

Running Head: RAC induced hypha branching in *Streptomyces* spp.

#Corresponding to: asamizu@g.ecc.u-tokyo.ac.jp (SA) and aonaka@g.ecc.u-tokyo.ac.jp (HO)

Abstract

Chemical cross talks between *Mycolicibacterium septicum* HEK138M and *Bacillus subtilis* 168 affect the bacterial morphology of *Streptomyces variegatus* HEK138A. We found that *S. variegatus* exhibits unusual hyphae branching by the bacterial interaction. We aimed to elucidate the mechanism by performing activity guided purification of substances that induce the unusual cell morphology. We found that pyrogallol, a redox active aromatic small molecule induced significant hyphae branching in *S. variegatus* and the activity was also observed in some of other *Streptomyces* species. Interestingly, the pyrogallol activity was diminished by adding catalase, which broke down H_2O_2. To further confirm the involvement, H_2O_2 was tested and similar activity which induced hyphal branching was observed. This indicates that reactive oxygen species (ROS) generated by redox-active compound (RAC) is the inducing factor of hyphae branching. Further investigation revealed that pyrogallol was generated by NahG enzyme homolog of *M. septicum* using 2,3-dihydroxybenzoic acid as substrate by heterologous expression in *E. coli*. Moreover, co-culture with gene knock-out mutants revealed that 2,3-dihydroxybenzoic acid was supplied by *B. subtilis* produced as intermediate of bacterial siderophore bacillibactin. Since the hyphae branching of vegetative mycelium can increase the density of filamentous network and consequently help secure the milieu in soil, our results suggested that those filamentous soil bacteria use ROS which can be supplied from plant derived RAC as a signal. As those RAC ubiquitously exist in soil environment, the system will be beneficial for sensing the nutrient

sources in addition to the generally considered defensive response to oxidative stress.

Importance

The characterization of interactions between three or more bacteria are lacking as these interactions are visually imperceptible in general. Our current study revealed changes of morphological behavior by the bacterial interaction. This study showed that hydrogen peroxide generated by redox-active compound derived from a breakdown product of siderophore can significantly increase the number of hyphae tip extension in filamentous bacteria. Our result implies the existence of oxidative response system using a low amount of reactive oxygen species as an integrated signal to sense the plant-derived carbon source by the filamentous soil bacteria. As a result of sensing, filamentous soil bacteria may decide whether the hypha tip should be extended to further explore the area or increase the tips to densify filamentous network to monopolize the nutrients in the milieu.

Introduction

Streptomyces species is an industrially important Gram-positive filamentous actinobacteria, which produces bioactive natural products (secondary metabolites: SMs) that can be used as antibiotics, pesticides, and anti-cancer drugs (1, 2). Actinomycetes including *Streptomyces* species can interact with mycolic acid-containing bacteria (MACB) such as *Tsukamurella pulmonis* TP-B0596; such bacterial interactions can have effects on the production of specialized metabolites by actinomycetes, refer to as combined-culture (3-5). MACB can activate the production of undecylprodigiosin in *Streptomyces lividans* TK23, which are not produced by this strain under general laboratory culture conditions (3, 6). Although the mechanism of induced production of SMs is yet to be elucidated (7), interactions among *Streptomyces* species and MACB likely occur naturally since the combination of these two species has been co-isolated from environmental soil (8). These observations evoke interests around the function of bacterial (secondary) metabolism for constructing the microbial community in a soil environment where *Streptomyces* species and MACB exist simultaneously.

MACB are a group of actinomycetes that contain specific long-chain fatty acids (C_{30}–C_{60} mycolic acids) in the cell wall (9). MACB has intrinsic resistance to antibiotics, which is conferred by the characteristic mycobacterial cell wall to avoid the penetration by antibiotics (10). Although the profit for *Streptomyces* species in this combination is obscure, these properties of MACB, inducer of SMs and resistance to antibiotics, can be considered to be responsible for the “combined” action of *Streptomyces*

bacteria and MACB to fight against the third party. Previous studies have reported several cases of pairwise interactions using SMs that involve additional third party (11, 12). For example, the association of fungus-growing leafcutter ants with actinomycetes has been previously reported. Leafcutter ants cultivate fungal gardens (of *Leucoagaricus* sp.) as a food source, but they are constantly threatened by invasive fungal species, such as *Escovopsis* sp. To compete against the invasive fungi, the ants also carry actinomycetes associates that produce antifungal SMs (e.g., candicidin D, nystatin, and dentigerumycin). Knowledge of visually perceptible interactions among more than three organisms is relatively well accumulated, however the interactions among three or more bacteria are largely unexplored as they are generally imperceptible in a cell size scale.

Streptomyces species have a complex life cycle unlike other bacteria that undergo binary fission. Their life cycle begins with a spore, and its germination initiates with the emergence of a germ tube. The germ tube extends by filamentous cell, which extends using polar tip to yield long hyphal filaments, and occasionally hyphal branches emerge from the trunk filament. This cell growth manner with the branching of hyphae leads to the formation of a filamentous cell network in vegetative growth phase (13, 14). Tip extended filamentous cells further undergo cell differentiation to aerial mycelium and then proceed cell division forming spore to complete life cycle. Unique example has been known such as exploratory growth of *Streptomyces* species by significant polar tip extension, which is induced by alkalized condition caused by fungi (15). However, as *Streptomyces* species has evolved complex

response system for diverse stimuli that can be derived from environment including bacterial interaction (16), what we have observed so far for morphological behavior would be only a limited fraction and large parts are remain unrevealed.

In a previous study, we found a natural combination of *Streptomyces* species and MACB that were co-isolated from environmental soil collected at Hegura Island, which involved alteration of secondary metabolism (8). In the combination that was retrieved, extracts from combined-culture among *S. variegatus* HEK138A and MACB: *Mycolicibacterium septicum* HEK138M showed specific antibacterial activity against Gram-positive bacteria, such as *Bacillus subtilis*. In the present study, we aimed to investigate the intergeneric interaction among *Streptomyces* species, MACB, and *B. subtilis*. By analyzing the phenotypic changes in the interaction area using scanning electron microscopy, we found abnormal cell shape formed in mycelia of *S. variegatus* HEK138A. Here, we report the characterization of metabolic interactions that generate redox active small molecule, which cause the induction of the disordered hyphal branch in *Streptomyces* species.

Results

Disordered hyphae branching of S. variegatus by bacterial interaction

S. variegatus HEK138A and *M. septicum* HEK138M was co-isolated from soil sample collected in Hegura island, Japan (8). Extracts from the combined-culture of these two species showed specific antibacterial activity against Gram-positive bacteria such as *B. subtilis* (8). We developed dual culture of *S. variegatus* and *M. septicum* to investigate whether the specific growth inhibition of *B. subtilis* can be observed on agar plate, as has been previously reported for the other combinations (5). In addition, we also investigated the phenotypic changes in the interaction area by scanning electron microscopy (SEM) to capture changes that were visually imperceptible. We noticed the slight color change at the edge of *S. variegatus* colony on agar plate culture (Fig. 1a). The cell morphological differentiation (aerial mycelium formation or spore formation) in *S. variegatus* was likely induced by chemical modulators that were produced as a result of bacterial interactions. This speculation was based on the fact that some natural products are known to change the cell differentiation of *Streptomyces* species (17-19). However surprisingly, the SEM image of the *S. variegatus* mycelium at the interaction area did not show the cells of developed morphology with aerial mycelium; instead, they showed irregular form of the vegetative mycelium (Fig. 1b). The mycelium observed using SEM showed disorderly emergence of hyphae branches; significant number of hyphae tip emerged from trunk mycelia (Fig. 1c-d).

Small molecules generated by bacterial interaction induce disordered hyphae branching

We first investigated which bacteria of two (*M. septicum* or *B. subtilis*) can induce the formation of disordered hyphae branching on mycelium of *S. variegatus*. Interestingly, the competitive dual culture did not induce the disordered hyphae branching on the mycelium of *S. variegatus* that was comparable to those of the triple-culture (Fig. S1). This indicates that the induction of disordered hyphae branching require the interactions between both *M. septicum* and *B. subtilis*. Thereafter, we tested whether organic substance(s) can induce the disordered hyphal branching of *S. variegatus* mycelium. For this, the triple-culture (solid) of *S. variegatus*, *M. septicum*, and *B. subtilis* was extracted using butanol and spotted next to the colony of *S. variegatus* that was grown on agar plate. After incubation, the *S. variegatus* colony was fixed for SEM imaging. The SEM image showed that substance(s) that was extracted using butanol can induce the emergence of similar disordered hyphae on the mycelium similar to those observed at the bacterial interaction area (Fig. 1f). We additionally analyzed the activity using slide culture, and the induction of hyphae branch by the culture extracts was also observed under a differential interference contrast microscope (DICM) (Fig. 1j). It was first presumed that bacitracin produced by *B. subtilis* was involved in the disordered hyphae emergence on mycelium of *S. variegatus* (20). However, this possibility was eliminated as *B. subtilis* 168 used in the experiment lacked bacitracin biosynthetic gene cluster and cannot produce bacitracin (21). Hence, in the present study, we performed purification to identify the active substance(s) that induce the hyphal branching.

Bioactivity guided isolation of substance that induce disordered hyphae branching

Triple-culture (liquid) of the three strains were extracted using ethyl acetate and the active substances were further purified using column chromatography which was guided by hyphae branch inducing activity (Fig. S2 shows the purification scheme). The activity was confirmed by images of the colony obtained by SEM or those of slide culture under DICM. Interestingly, when the culture extracts were subjected to Sephadex LH20 column chromatography, activity was observed in two different fractions (No. 7 and 9) (Fig. S3). Both active fractions were further subjected for purification, but low yield and poor chemical signature of the substance(s) from the fraction No. 9 prevented further isolation of the compound. Therefore, we focused on the substance obtained from fraction No. 7 and further purified by open ODS column and preparative high-performance liquid chromatography (HPLC), and successfully isolated the active compound. The spectral data (HR-ESI-QTOF-MS, ^{1}H NMR, and ^{13}C NMR) of the purified compound contained chemical shifts that were identical to a compound known as pyrogallol. ^{1}H NMR: 6.31 (2H, d, *J*=8.0), 6.49 (1H, t, *J*=8.2); ^{13}C NMR: 147.3, 134.5, 120.2, 108.4; HR-MS: obs. 127.0395 $[M+H]^{+}$ (calc. 127.0390 $[M+H]^{+}$ for molecular formula of $C_6O_3H_7^{+}$) (Fig. S4, Table S1). Hence, commercially available pyrogallol was used for further experiments.

Effect of pyrogallol against S. variegatus*, *M. septicum*, and *B. subtilis

Pyrogallol is known as inhibitor of bacterial growth (22). Hence, we first determined the

concentration of pyrogallol that show the growth inhibition using agar medium assay. We found that 32 μg/ml of pyrogallol can completely inhibit the growth of *S. variegatus* and *M. septicum*; *B. subtilis* showed relatively high tolerance to pyrogallol (inhibition concentration: 256 μg/ml) (Table S2). Subsequently, different concentrations of pyrogallol (0.1, 1, and 10 μM) were tested against *S. variegatus* and activity of hyphae branching was observed under DICM. Obtained image confirmed that pyrogallol can consistently and reproducibly induce the hyphae branching (Fig. S5a). However, when the SEM images of the bacterial interaction area and of the area in presence of pyrogallol were compared (Fig. 1d and 1g), slightly different images were obtained. The mycelium at the interaction area was rich in saccular-like structure with smooth surface (Fig. 1d). In contrast, the presence of pyrogallol resulted in rough surface with rather deformed cells (Fig. 1g). This difference in morphology maybe attributed to the presence of at least two substances in the culture extract that can induce the abnormal cell form (Fig. S3). Thus, mixture of these substances may be responsible for the cell morphology observed at the interaction area. Although the SEM image showed slightly different morphology, slide culture images showed the clear and significant emergence of hyphae branch (Fig. 1k and S4a), strongly indicating that addition of pyrogallol induce hyphae branching.

Pyrogallol induced hyphae branching in a broad range of Streptomyces species

Subsequently, to investigate whether pyrogallol can induce hyphae branching in other

170 *Streptomyces* species, same concentrations of pyrogallol was tested for six other *Streptomyces* species

171 that are generally used for biological experiments. Similar to the mycelium of *S. variegatus*, the mycelia

172 of *S. griseus* IFO13350, *S. albus* J1046, and *S. lividans* TK23 showed significant emergence of hyphae

173 branch in all concentrations consistently and reproducibly (Fig. S5b-d). *S. venezuelae* NBRC13096 and

174 *S. avermitilis* MA4680 receive similar effect, but was weaker than that observed in *S. variegatus* (Fig.

175 S5e-f). The tested concentration did not show the expected phenotypic changes in *S. coelicolor* A3(2)

176 M145 (Fig. S5g); however, the reason is not clear yet. Additionally, effects of pyrogallol (10 μM) for *M.*

177 *septicum* and *B. subtilis* was also tested, which showed that most of the *B. subtilis* cells showed ordinary

178 shape, but several cells also showed round shape rather than rod shape (23) (Fig. S6a), and *M. septicum*

179 sustained no apparent phenotypic change (Fig. S6b).

180

181 ***Quantification of lengths of tip-to-branch and branch-to-branch***

182 As *S. griseus* showed similar response by addition of pyrogallol to *S. variegatus* (Fig. S5a-b),

183 We further used *S. griseus* to evaluate the quantitative significance of the inducing activity of hyphae

184 branch by pyrogallol. AcGFP1 was expressed in *S. griseus* (*S. griseus::Acgfp1*) to illuminate the

185 mycelium. The images of slide culture were obtained under confocal laser scanning microscope (CLSM).

186 We used fluorescence excitation (488 nm) and emission (510 nm) wavelength to confirm that AcGFP1 is

187 expressed in every mycelium. It was observed that mycelium cells were thoroughly illuminated by

188 fluorescence AcGFP1 (Fig. S7). After obtaining the multiple images of CLSM, we performed image
189 extraction, disassemble process, and length measurement using ImageJ (Fiji), which was employed in
190 JAVA-based WEKA platform (24). We disassembled the image of the grown hyphae, and lengths of the
191 tip-to-branch and branch-to-branch were measured to obtain the quantitative data. Lengths of the
192 tip-to-branch and branch-to-branch were used for criterion to define the frequency of hyphae branch.
193 The addition of 1 μM pyrogallol significantly reduced the length of tip-to-branch (0.71-fold) by
194 comparing the median value (3.08 nm by addition of pyrogallol and 5.32 nm in control) ($p=4.34\times10^{-9}$)
195 (Fig. 2b-c and 2g left). Additionally, the length of branch-to-branch also reduced significantly
196 (0.71-fold) by comparing the median value (8.17 nm by addition of pyrogallol and 11.47 nm in control)
197 ($p=1.27\times10^{-7}$) as well (Fig. 2g right). The result confirmed that pyrogallol induces the generation of
198 short mycelium in high frequency.
199
200 ***Hydrogen peroxide generated by pyrogallol induced hyphae branching***
201 Catechol (*ortho*-hydroxyphenol) or quinol (*para*-hydroxyphenol) is well characterized as RAC,
202 which can react with molecular oxygen to be oxidized and form (*ortho*- or *para*-) quinone, and readily
203 generate oxide such as hydrogen peroxide (H_2O_2) (25). Therefore, we hypothesized that the H_2O_2 can
204 induce the emergence of hyphae branching in mycelium of *Streptomyces* species since chemically
205 similar effect can be applied for pyrogallol (Fig. 2a) (26). To test this hypothesis, we first added catalase

to the culture medium containing 1 μM pyrogallol to breakdown the generated H_2O_2. Catalase can convert two molecules of H_2O_2 to two molecules of H_2O and one molecule of O_2 to detoxify the oxidative stress (Fig. 2a) (27). *S. griseus::Acgfp1* was cultured in catalase-containing medium with or without pyrogallol, and further hyphae lengths were measured. The result showed that the emergence of hyphae branch which was expected to be induced by pyrogallol was almost abolished by addition of 22 U/ml of catalase (Fig. 2d-e). The quantification analysis showed that lengths of both tip-to-branch and branch-to-branch have no significant differences in lengths in presence of catalase (p-value=0.299 and p-value=0.014, respectively) (Fig. 2h). The result revealed that activity of pyrogallol was quenched by catalase which decompose H_2O_2. To further verify the involvement of H_2O_2 as an inducer of hyphae branch, we then added H_2O_2 to the culture of *S. griseus::Acgfp1*. By adding 0.88 μM of H_2O_2, we notably observed the similar phenotype comparable to addition of pyrogallol, which the emergence of hyphae was induced (Fig. 2b-c and 2f). The result of quantification supported the significant emergence of hyphae by the values that both length of tip-to-branch and branch-to-branch become shorter (0.84-fold and 0.69-fold, respectively) with significance (p-value=4.51×10^{-4} and p-value=1.80×10^{-5}, respectively) by addition of H_2O_2 (Fig. 2i). The result revealed that H_2O_2 generated by pyrogallol is the signal to induce emergence of hyphae branch.

Pyrogallol was generated by M. septicum from 2,3-DHBA supplied by B. subtilis

To identify the producer(s) of the pyrogallol, we cultured *S. variegatus*, *M. septicum*, and *B. subtilis* in possible combinations and analyzed the extracted metabolites using HPLC equipped by photodiode array (PDA). PDA-HPLC traces showed that pyrogallol was produced in co-culture of *M. septicum* + *B. subtilis* (930 ± 40 μM) and triple-culture of *S. variegatus* + *M. septicum* + *B. subtilis* (100 ± 40 μM), indicating that *S. variegatus* is not directly involved in the production of pyrogallol (Fig. 3b and S8). Previous studies showed that gallic acid (28) or 2,3-DHBA (29) can be a direct precursor of pyrogallol by microbial conversion. Therefore, we tested the conversion by feeding gallic acid (0.5 mM) or 2,3-DHBA (0.25 mM) to the culture of *M. septicum* or *B. subtilis*. HPLC traces revealed that pyrogallol was formed only when 2,3-DHBA was fed to the culture of *M. septicum* with yield of 37.3 ± 9.8 μM (14.9% conversion rate) (Fig. 3c and S9). It is known that *B. subtilis* produces 2,3-DHBA as an intermediate of its siderophore, bacillibactin (30) (Fig. 3a). Hence, we hypothesized that 2,3-DHBA secreted by *B. subtilis* was supplied to *M. septicum* as a precursor of pyrogallol. To test this, we co-cultured *M. septicum* with knock-out mutants of the bacillibactin biosynthetic genes (*dhbA-F*) of *B. subtilis* (30, 31). When *M. septicum* was co-cultured with *B. subtilis* Δ*dhbF* or Δ*dhbE,* both of which can accumulate 2,3-DHBA as intermediate, pyrogallol was detected in the co-culture broth (Fig. 3d and S10). In contrast, when *M. septicum* was co-cultured with Δ*dhbC*, Δ*dhbB* or Δ*dhbA* strains which cannot accumulate 2,3-DHBA, pyrogallol was not detected (Fig. 3d and S10). Generation of pyrogallol was consistent with the availability of 2,3-DHBA in the blocked mutants. Notably, the result demonstrated

that 2,3-DHBA, bacillibactin biosynthesis intermediate, was direct precursor of pyrogallol synthesis by *M. septicum*.

Salicylate 1-monooxygenase (NahG) from M. septicum convert 2,3-DHBA to pyrogallol

As pyrogallol was synthesized from 2,3-DHBA by *M. septicum*, we searched the enzyme that convert 2,3-DHBA to pyrogallol. Previously, *nahG* (salicylate 1-monooxygenase, EC 1.14.13.1) from *Pseudomonas putida* DOT-T1E was reported to convert 2,3-DHBA to pyrogallol using *E. coli* as host (29). Draft genome sequence of *M. septicum* was obtained, and a possible $NahG^{Ms}$ enzyme with 31% similarity in deduced amino acid were found (Fig. S11). The $nahG^{Ms}$ was cloned and expressed under T7 promoter in *E. coli* BL21(DE3) (Fig. 4a). Using *E. coli* resting cell expressing the $NahG^{Ms}$, we incubated 2,3-DHBA or salicylate (as native precursor) and traced the conversion using PDA-HPLC. As expected, generation of pyrogallol from 2,3-DHBA (Fig. 4b-e), as well as catechol from salicylate (Fig. S12) was observed only in the reaction with *E. coli* resting cell expressing the $NahG^{Ms}$. Hence, it was revealed that NahG enzyme from *M. septicum* can accept 2,3-DHBA as well as salicylate as substrate and catalyze oxidative decarboxylation to produce pyrogallol or catechol.

Estimation of the distribution of 2,3-DHBA and nahG homolog in soil environment

Several bacterial species are known to produce siderophore with catechol units, whose

precursor is 2,3-DHBA (32). We searched for the orthologous gene set that is responsible for the production of 2,3-DHBA, which comprise *dhbC* (isochorismate synthase), *dhbB* (isochorismate lyase domain), and *dhbA* (2,3-dihydro-2,3-dihydroxybenzoate dehydrogenase) using KEGG database. We found that 10.6% (789/7393) of bacterial strains possessed the gene set, and remarkably, percentile was 84.7% (111/131) in *Bacillus* species. This bioinformatic result implies that 2,3-DHBA abundantly exist in the soil bacterial community. We then searched for the *nahG* ortholog gene in MACB (such includes *Tsukamurella*, *Rhodococcus*, *Corynebacterium*, *Gordonia*, and *Nocardia* spp.). It was found that 18.1% (28/155) of MACB possessed the *nahG* ortholog, and percentile was 10.5% (4/38) for *Mycolicibacterium* species. Overall, the result implied that our observation of significant emergence of hypha branch on mycelium of *Streptomyces* species by pyrogallol may stochastically occur in the environmental bacterial soil community.

Discussion

Our study revealed that pyrogallol was a decomposed product derived from the assembly component for catechol-type siderophore. This metabolic interaction between MACB and *Bacillus* species likely represents the competition for acquiring iron from the environment. Our present study also identified that redox active compound (RAC) such as pyrogallol, can modulate cell morphology of *Streptomyces* species *via* generation of reactive oxygen species (ROS) such as H_2O_2 (Fig. 5). Interaction involving bacteria observed in our current study may stochastically occur in the soil environment, however, our observation also suggested the general behavior of filamentous bacteria against oxidative signals.

SMs that affect the morphological behavior of Streptomyces species

Several SMs from *Bacillus* species have been reported to show intergeneric chemical communications between *Streptomyces* and *Bacillus* species. *B. subtilis* produces surfactin, which is a lipopeptide antibiotic that inhibits the formation of aerial hyphae of streptomycetes by defecting the hydrophobic cell wall (33). *B. subtilis* also produces bacillaene, NRP/PK hybrid compound, that inhibits the production of undecylprodigiosin by *S. coelicolor* A3(2) (34). As described before, bacitracin modulates the emergence of hyphae by inducing the phosphorylation of DivIVA protein (20). Additionally, several other examples of interspecies or intergeneric chemical cross talk have been previously reported. Desferrioxamines, which is bacterial siderophore described as public goods for ion

acquisition, can be donated by a bacteria species; it affects the cell differentiation and antibiotic production of receiver *Streptomyces* species (35). Furthermore, several specific SMs have been reported to induce aerial mycelium, such as hormaomycin (19) (or takaokamyicin) (36) from *S. griseoflavus* W-384 and panamycin-607 (37) from *S. alboniger* IFO 12738. In sublethal concentrations, goadsporin (17) and lincomycin (38) affect both secondary metabolism and morphological differentiation in other actinomycetes. In addition to the previously known bacterial strain specific specialized SMs, our findings identified that pyrogallol which is more generally exist in the environment modulate cell morphology of *Streptomyces* species. This likely suggest that *Streptomyces* species has evolved unsolved response systems for more general stimuli in the environment.

Signals for hypha branch in Streptomyces species

Hyphae branching of vegetative mycelium can be beneficial as it increases the density of filamentous cell network, which can help secure the milieu in soil environment. However, knowledge of the mechanisms how to determine the points of hyphal tip emergence (or polarisome) in *Streptomyces* species is still unknown. Hypha extension and hyphal branching involves two coiled-coil proteins, namely DivIVA (39) and Scy (40), which form protein complexes described as polarisomes as well as intermediate filament-like protein FilP (41) that interacts with the polarisome. The DivIVA is essential for recruiting the two coiled-coil proteins, whereas Scy colocalizes with DivIVA to construct scaffold in the polarisome and FilP provides mechanical support by forming a stress bearing network behind the

309 hyphal tip. Partial or null deletion or overexpression of the genes can affect the tip extension and hyphae
310 branching (42), indicating that modulation of the polarisomes can disturb the extension of polar tip of
311 the hyphae. Excessive phosphorylation of DivIVA by a bacterial serine/threonine kinase AfsK can
312 modulate the polar extension and branching, particularly in response to inhibitors of cell wall synthesis,
313 such as bacitracin and vancomycin (20). Co^{2+}-binding bacitracin binds tightly to the undecaprenyl
314 pyrophosphate, which interferes with cell wall synthesis by preventing its hydrolysis to monophosphate,
315 which is essential step in peptidoglycan biosynthesis (43). In addition, osmotic challenge can also induce
316 hyphal branching in *S. coelicolor* M145 (44). However, mechanism which direct the emergence of
317 hyphae in the high osmotic shift challenge is yet unknown. Although future studies should be required to
318 identify the mechanism by which disturbance of polarisome is involved in disordered hyphae branching
319 by H_2O_2, our present study newly demonstrated that H_2O_2 generated by RAC become a diving force for
320 the emergence of hypha branch.

321 ***Response system for ROS in Streptomyces species***

322 Pyrogallol can generate ROS including H_2O_2 by conversion to its *ortho*-(benzo)quinone form.
323 Recently, several SMs including actinorhodin (45) or granaticin (46) have been revealed as RAC that
324 generate H_2O_2. Although the molecular response regulation of *Streptomyces* species in response to
325 oxidative stress is relatively well characterized (47), ROS-induced emergence of hypha has not been
326 described. The ability to respond to oxidative stress is critical for survival, and organisms have evolved

327 diverse strategies to sense oxidative stress. When face with direct oxidative challenge in the environment,
328 bacteria exercise a system to detoxify oxidants such as super oxide anion (O^{2-}) and hydrogen peroxide
329 (H_2O_2) by using two major regulatory protein, SoxR to induce superoxide dismutase (48) and OxyR to
330 induce catalase (49), which is also conserved in *Streptomyces* species. The principal oxidative stress
331 response in *Streptomyces* is controlled by a regulatory system consisting of a σ-factor SigR (47, 50), and
332 a redox-sensitive anti-σ-factor, RsrA (51). The RsrA is a Zn^{2+} binding protein that binds to SigR with
333 nanomolar affinity under reducing conditions, which prevents it from associating with RNA polymerase
334 to activate transcription. When the cell encounters oxidative stress, an intramolecular disulfide bond
335 forms between two of the cysteines, leading to expulsion of Zn^{2+} and inactivation of RsrA. Thereafter,
336 SigR is released, which activates the transcription of a regulon consisting of more than 100 target genes.
337 Regulon of SigR was investigated using ChiP-seq and revealed 108 regulons (52). In our search, the
338 SigR regulon did not include genes involved in the hyphae tip extension such as DivVIA (*sco2077*), Scy
339 (*sco5397*), FilP (*sco5396*), noncoiled-coil protein MreB (*sco2611*), FtsZ (*sco2082*), other coiled-coil
340 protein *sco3114* and *sco2168*. Therefore, known principle of oxidative stress response involving
341 SigR/RsrA or OxyR/SoxR in *Streptomyces* species may not directly be involved in the induced
342 emergence of hyphae branch.

343 ***Bacterial behavior in soil ecosystem***

344 Though ROS are injurious by-products, they are essential participants in cell signaling and

regulation in low concentrations (53). In soil, bacteria decompose plant components such as gallic acid, ellagic acid, tannic acid, and lignin that contain redox active groups (54), and those are used as carbon source for the growth of actinobacteria. Pyrogallol or catechol component which can generate low amount of H_2O_2 are decomposed products of those. Meanwhile emergence of hyphae branching can be considered to increase the density of filamentous network of *Streptomyces* species. Using low amount of H_2O_2 as an integrated signal to sense (recognize) the plant derived carbon source can be beneficial for the filamentous bacteria. Existence of those system can likely help decide whether to extend tip to explore more area or to increase the density of filamentous network to construct exclusive area which can take advantage of *Streptomyces* species to monopolize the nutrients.

Materials and methods

General

S. variegatus HEK138A and *M. septicum* HEK138M were isolated from Hegura Island in Japan, and the taxonomy of the strains were identified based on the 16S rDNA sequences (8). The culture conditions of *S. lividans* TK23, *S. griseus* IFO 13350, *S. avermitilis* MA-4680, *S. coelicolor* A3(2) M145 *S. venezuelae* NBRC13096, and *S. albus* J1046 followed the standard protocol (55). *B. subtillis* 168 and the BKE library (BKE32000, BKE31970, BKE31990, BKE31980, BKE31960) used in the present study were obtained from National BioResource Project (NIG, Japan). Additional information can be found in *Supplemental Material*.

Acknowledgments:

This research was supported by a grant-in-aid from the Institute for Fermentation, Osaka, (IFO) and Amano Enzyme Foundation (to S.A. and H.O.). This study was also partially supported by KAKENHI research grants (18K05385 to S.A. and 18H02120 to H.O.), general research grant from IFO (to S.A.), general research grant from Noda institute for scientific research (to S.A.), and the JSPS A3 Foresight Program. M.K. is supported by JST SPRING GX program. We thank Prof. Yasuo Ohnishi and Dr. Takeaki Tezuka for the AcGFP1 plasmid and technical supports in *S. griseus* genetic experiments. *Bacillus subtillis* BKE library were obtained from National BioResource Project (NIG, Japan). All authors declare no conflicts of interest associated with this manuscript. All authors designed research and analyzed data. M.K. performed all experiments. S.A. wrote the main text, M.K. and S.A. prepared figures and tables, and H.O. review the manuscript.

380 References

381 1. Newman DJ, Cragg GM. Natural Products as Sources of New Drugs over the Nearly Four Decades from

382 01/1981 to 09/2019. J Nat Prod. 2020;83(3):770-803.

383 2. Van der Meij A, Worsley SF, Hutchings MI, van Wezel GP. Chemical ecology of antibiotic production

384 by actinomycetes. Fems Microbiology Reviews. 2017;41(3):392-416.

385 3. Onaka H, Mori Y, Igarashi Y, Furumai T. Mycolic Acid-Containing Bacteria Induce Natural-Product

386 Biosynthesis in Streptomyces Species. Appl Environ Microb. 2011;77(2):400-6.

387 4. Hoshino S, Onaka H, Abe I. Activation of silent biosynthetic pathways and discovery of novel

388 secondary metabolites in actinomycetes by co-culture with mycolic acid-containing bacteria. J Ind

389 Microbiol Biotechnol. 2019;46(3-4):363-74.

390 5. Asamizu S, Pramana AAC, Kawai SJ, Arakawa Y, Onaka H. Comparative Metabolomics Reveals a

391 Bifunctional Antibacterial Conjugate from Combined-Culture of Streptomyces hygroscopicus HOK021 and

392 Tsukamurella pulmonis TP-B0596. Acs Chem Biol. 2022;17(9):2664-72.

393 6. Asamizu S, Ozaki T, Teramoto K, Satoh K, Onaka H. Killing of Mycolic Acid-Containing Bacteria

394 Aborted Induction of Antibiotic Production by Streptomyces in Combined-Culture. Plos One.

395 2015;10(11):e0142372.

396 7. Yanagisawa M, Asamizu S, Satoh K, Oono Y, Onaka H. Effects of carbon ion beam-induced mutagenesis

397 for the screening of RED production-deficient mutants of Streptomyces coelicolor JCM4020. Plos One.

398 2022;17(7):e0270379.

399 8. Kato M, Asamizu S, Onaka H. Intimate relationships among actinomycetes and mycolic acid-containing

400 bacteria. Sci Rep. 2022;12(1):7222.

401 9. Jankute M, Cox JAG, Harrison J, Besra GS. Assembly of the Mycobacterial Cell Wall. Annu Rev

402 Microbiol. 2015;69:405-23.

403 10. Gygli SM, Borrell S, Trauner A, Gagneux S. Antimicrobial resistance in Mycobacterium tuberculosis:

404 mechanistic and evolutionary perspectives. FEMS Microbiol Rev. 2017;41(3):354-73.

405 11. Scherlach K, Hertweck C. Chemical Mediators at the Bacterial-Fungal Interface. Annual Review of

406 Microbiology, Vol 74, 2020. 2020;74:267-90.

407 12. Batey SFD, Greco C, Hutchings MI, Wilkinson B. Chemical warfare between fungus-growing ants and

408 their pathogens. Curr Opin Chem Biol. 2020;59:172-81.

409 13. Szafran MJ, Jakimowicz D, Elliot MA. Compaction and control-the role of chromosome-organizing

410 proteins in Streptomyces. FEMS Microbiol Rev. 2020;44(6):725-39.

411 14. Barka EA, Vatsa P, Sanchez L, Gaveau-Vaillant N, Jacquard C, Meier-Kolthoff JP, et al. Taxonomy,

412 Physiology, and Natural Products of Actinobacteria (vol 80, pg 1, 2016). Microbiol Mol Biol R.

413 2016;80(4):Iii-Iii.

414 15. Jones SE, Ho L, Rees CA, Hill JE, Nodwell JR, Elliot MA. Streptomyces exploration is triggered

415 by fungal interactions and volatile signals. Elife. 2017;6.

416 16. Zambri MP, Williams MA, Elliot MA. How Streptomyces thrive: Advancing our understanding of
417 classical development and uncovering new behaviors. Adv Microb Physiol. 2022;80:203-36.
418 17. Onaka H, Tabata H, Igarashi Y, Sato Y, Furumai T. Goadsporin, a chemical substance which promotes
419 secondary metabolism and morphogenesis in streptomycetes - I. Purification and characterization. J
420 Antibiot. 2001;54(12):1036-44.
421 18. Kondo S, Yasui K, Natsume M, Katayama M, Marumo S. Isolation, physico-chemical properties and
422 biological activity of pamamycin-607, an aerial mycelium-inducing substance from Streptomyces alboniger.
423 J Antibiot (Tokyo). 1988;41(9):1196-204.
424 19. Andres N, Wolf H, Zahner H, Rossner E, Zeeck A, Konig WA, et al. Hormaomycin, a Novel Peptide
425 Lactone with Morphogenetic Activity on Streptomyces .252. Helv Chim Acta. 1989;72(3):426-37.
426 20. Hempel AM, Cantlay S, Molle V, Wang SB, Naldrett MJ, Parker JL, et al. The Ser/Thr protein kinase
427 AfsK regulates polar growth and hyphal branching in the filamentous bacteria Streptomyces. Proc Natl Acad
428 Sci U S A. 2012;109(35):E2371-9.
429 21. Steinke K, Mohite OS, Weber T, Kovacs AT. Phylogenetic Distribution of Secondary Metabolites in
430 the Bacillus subtilis Species Complex. Msystems. 2021;6(2).
431 22. Kocacaliskan I, Talan I, Terzi I. Antimicrobial activity of catechol and pyrogallol as
432 allelochemicals. Zeitschrift Fur Naturforschung Section C-a Journal of Biosciences. 2006;61(9-10):639-42.
433 23. Jones LJF, Carballido-Lopez R, Errington J. Control of cell shape in bacteria: Helical, actin-like

434 filaments in Bacillus subtilis. Cell. 2001;104(6):913-22.

435 24. Witten IH, Frank E, Hall MA, Pal CJ. The WEKA workbench. Data Mining: Practical Machine Learning

436 Tools and Techniques, 4th Edition. 2017:553-71.

437 25. Pinnataip R, Lee BP. Oxidation Chemistry of Catechol Utilized in Designing Stimuli-Responsive

438 Adhesives and Antipathogenic Biomaterials. Acs Omega. 2021;6(8):5113-8.

439 26. Marklund S, Marklund G. Involvement of the superoxide anion radical in the autoxidation of

440 pyrogallol and a convenient assay for superoxide dismutase. Eur J Biochem. 1974;47(3):469-74.

441 27. Nicholls P, Fita I, Loewen PC. Enzymology and structure of catalases. Adv Inorg Chem.

442 2001;51:51-106.

443 28. Kambourakis S, Draths KM, Frost JW. Synthesis of gallic acid and pyrogallol from glucose: Replacing

444 natural product isolation with microbial catalysis. J Am Chem Soc. 2000;122(37):9042-3.

445 29. Wang J, Shen XL, Yuan QP, Yan YJ. Microbial synthesis of pyrogallol using genetically engineered

446 Escherichia coli. Metab Eng. 2018;45:134-41.

447 30. May JJ, Wendrich TM, Marahiel MA. The dhb operon of Bacillus subtilis encodes the biosynthetic

448 template for the catecholic siderophore 2,3-dihydroxybenzoate-glycine-threonine trimeric ester

449 bacillibactin. Journal of Biological Chemistry. 2001;276(10):7209-17.

450 31. Koo BM, Kritikos G, Farelli JD, Todor H, Tong K, Kimsey H, et al. Construction and Analysis of

451 Two Genome-Scale Deletion Libraries for Bacillus subtilis. Cell Syst. 2017;4(3):291-305.

452 32. Kramer J, Oezkaya O, Kuemmerli R. Bacterial siderophores in community and host interactions. Nat
453 Rev Microbiol. 2020;18(3):152-63.
454 33. Straight PD, Willey JM, Kolter R. Interactions between Streptomyces coelicolor and Bacillus
455 subtilis: Role of surfactants in raising aerial structures. J Bacteriol. 2006;188(13):4918-25.
456 34. Vargas-Bautista C, Rahlwes K, Straight P. Bacterial Competition Reveals Differential Regulation
457 of the pks Genes by Bacillus subtilis. J Bacteriol. 2014;196(4):717-28.
458 35. Yamanaka K, Oikawa H, Ogawa HO, Hosono K, Shinmachi F, Takano H, et al. Desferrioxamine E produced
459 by Streptomyces griseus stimulates growth and development of Streptomyces tanashiensis. Microbiol-Sgm.
460 2005;151:2899-905.
461 36. Omura S, Mamada H, Wang NJ, Imamura N, Oiwa R, Iwai Y, et al. Takaokamycin, a new peptide antibiotic
462 produced by Streptomyces sp. J Antibiot (Tokyo). 1984;37(7):700-5.
463 37. Pogell BM. The pamamycins: Developmental autoregulators and antibiotics from Streptomyces
464 alboniger. A review and update. Cell Mol Biol. 1998;44(3):461-3.
465 38. Imai Y, Sato S, Tanaka Y, Ochi K, Hosaka T. Lincomycin at Subinhibitory Concentrations Potentiates
466 Secondary Metabolite Production by Streptomyces spp. Appl Environ Microb. 2015;81(11):3869-79.
467 39. Flardh K. Essential role of DivIVA in polar growth and morphogenesis in Streptomyces coelicolor
468 A3(2). Molecular Microbiology. 2003;49(6):1523-36.
469 40. Holmes NA, Walshaw J, Leggett RM, Thibessard A, Dalton KA, Gillespie MD, et al. Coiled-coil protein

470 Scy is a key component of a multiprotein assembly controlling polarized growth in Streptomyces. P Natl
471 Acad Sci USA. 2013;110(5):1580-1.
472 41. Bagchi S, Tomenius H, Belova LM, Ausmees N. Intermediate filament-like proteins in bacteria and
473 a cytoskeletal function in Streptomyces. Molecular Microbiology. 2008;70(4):1037-50.
474 42. Hempel AM, Wang SB, Letek M, Gil JA, Flardh K. Assemblies of DivIVA Mark Sites for Hyphal Branching
475 and Can Establish New Zones of Cell Wall Growth in Streptomyces coelicolor. J Bacteriol.
476 2008;190(22):7579-83.
477 43. Stone KJ, Strominger JL. Mechanism of Action of Bacitracin - Complexation with Metal Ion and
478 C55-Isoprenyl Pyrophosphate. P Natl Acad Sci USA. 1971;68(12):3223-+.
479 44. Fuchino K, Flardh K, Dyson P, Ausmees N. Cell-Biological Studies of Osmotic Shock Response in
480 Streptomyces spp. J Bacteriol. 2017;199(1).
481 45. Nishiyama T, Hashimoto Y, Kusakabe H, Kumano T, Kobayashi M. Natural low-molecular mass organic
482 compounds with oxidase activity as organocatalysts. P Natl Acad Sci USA. 2014;111(48):17152-7.
483 46. Nishiyama T, Enomoto N, Nagayasu R, Ueda K. Organocatalytic activity of granaticin and its
484 involvement in bactericidal function. Sci Rep-Uk. 2022;12(1).
485 47. Park JH, Lee JH, Roe JH. SigR, a hub of multilayered regulation of redox and antibiotic stress
486 responses. Molecular Microbiology. 2019;112(2):420-31.
487 48. Lee KL, Singh AK, Heo L, Seok C, Roe JH. Factors affecting redox potential and differential

488 sensitivity of SoxR to redox-active compounds. Molecular Microbiology. 2015;97(5):808-21.

489 49. Hahn JS, Oh SY, Roe JH. Role of OxyR as a peroxide-sensing positive regulator in Streptomyces

490 coelicolor A3(2). J Bacteriol. 2002;184(19):5214-22.

491 50. Paget MSB, Kang JG, Roe JH, Buttner MJ. sigma(R), an RNA polymerase sigma factor that modulates

492 expression of the thioredoxin system in response to oxidative stress in Streptomyces coelicolor A3(2).

493 Embo J. 1998;17(19):5776-82.

494 51. Kang JG, Paget MSB, Seok YJ, Hahn MY, Bae JB, Hahn JS, et al. RsrA, an anti-sigma factor regulated

495 by redox change. Embo J. 1999;18(15):4292-8.

496 52. Kim MS, Dufour YS, Yoo JS, Cho YB, Park JH, Nam GB, et al. Conservation of thiol-oxidative stress

497 responses regulated by SigR orthologues in actinomycetes. Molecular Microbiology. 2012;85(2):326-44.

498 53. Sies H, Jones DP. Reactive oxygen species (ROS) as pleiotropic physiological signalling agents.

499 Nat Rev Mol Cell Bio. 2020;21(7):363-83.

500 54. Shin M, Park E, Lee H. Plant-Inspired Pyrogallol-Containing Functional Materials. Adv Funct Mater.

501 2019;29(43).

502 55. Kieser T, Bibb MJ, Buttner MJ, Chater KF, Hopwood DA. Practical Streptomyces Genetics: John Innes

503 Foundation; 2000.

504

505

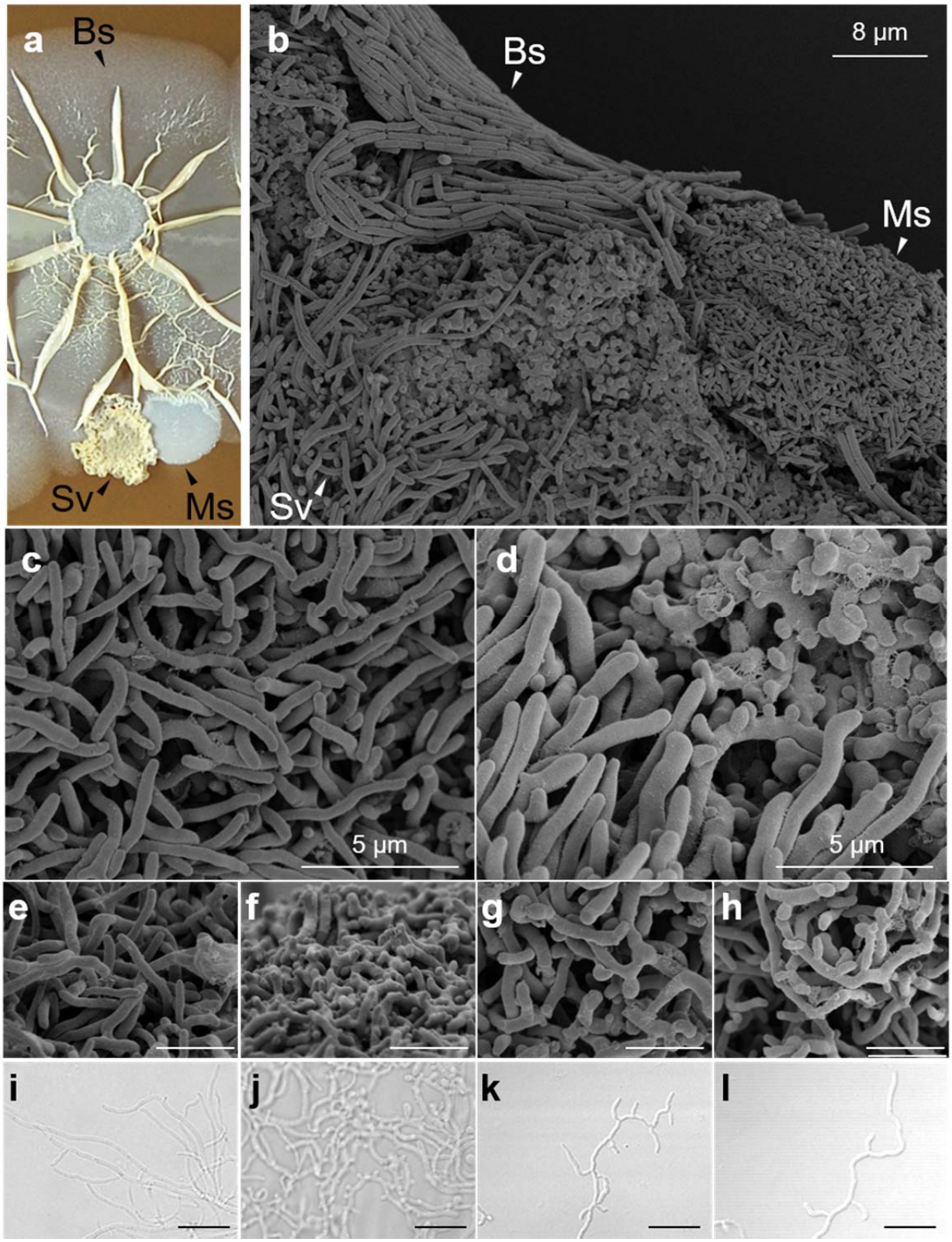

506 **FIG 1** Disordered hyphae branching of *S. variegatus*. (a) Triple-culture of Sv, Ms, and Bs on agar plate.

(b) SEM image of the interaction area of Sv, Ms, and Bs. (c) Magnified SEM image of normally grown Sv mycelium on agar plate. (d) Magnified SEM image of Sv mycelium at the interaction with Ms and Bs on agar plate. SEM images of colony (e-h) and DICM images of mycelium grown in slide culture (i-l). Morphology of normally grown *S. variegatus* cell (e, i); morphology of *S. variegatus* cell by addition of butanol extract from triple-culture (f, j); by addition of authentic pyrogallol (g, k); and by addition of H_2O_2 (h, j). Sv: *S. variegatus* HEK138A; Ms: *M. septicum* HEK138M; Bs: *B. subtilis* 168. (scale bar: 5 μm for a-d and 10 μm for e-h)

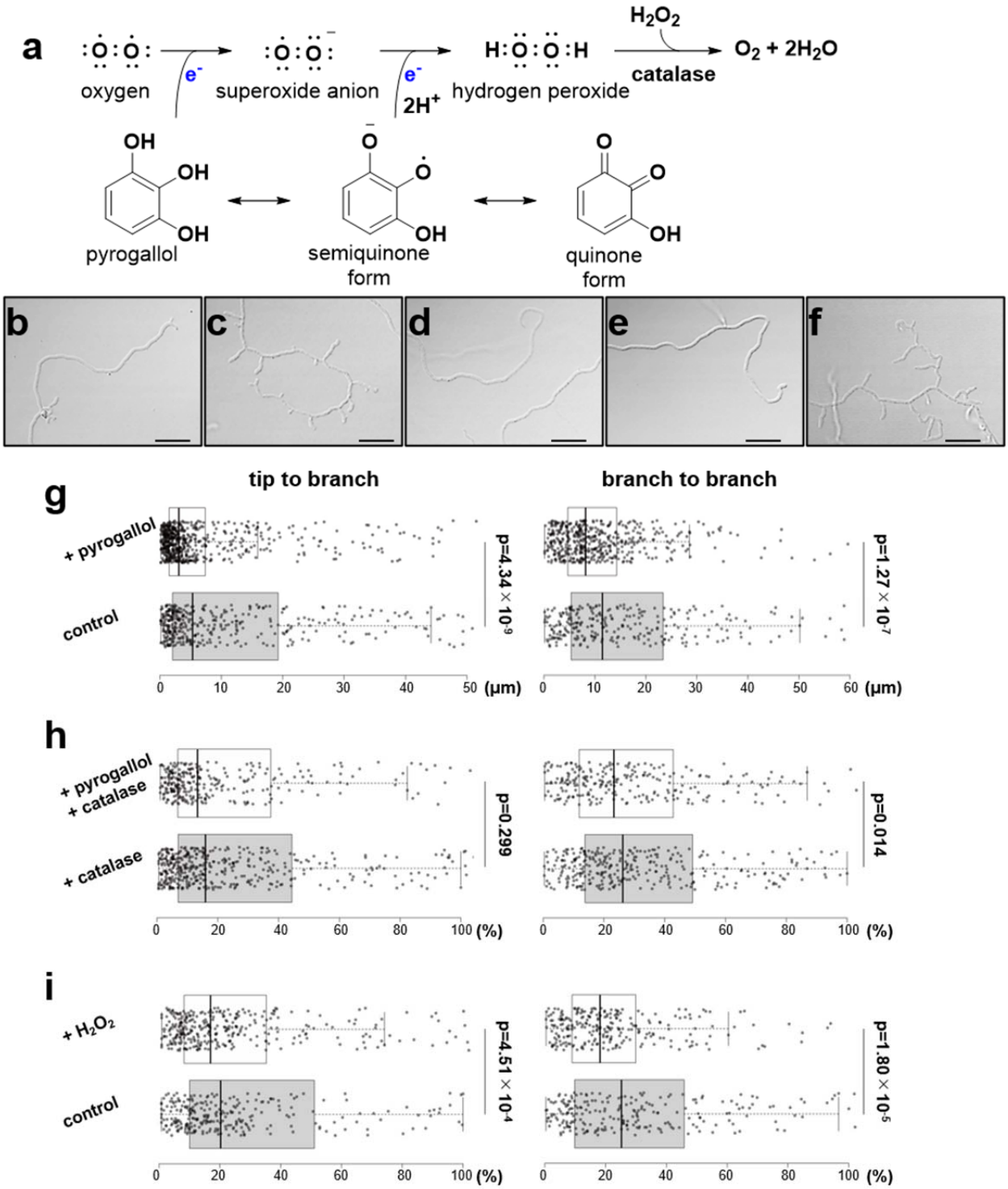

515 **FIG 2** Disordered hyphae branching of *S. variegatus* induced by H_2O_2 generated from RAC. (a)

516 Reaction scheme of pyrogallol (RAC) to generate H_2O_2 (ROS). (b-e) DICM images of *S. griseus*

517 IFO13350 (AcGFP1) mycelium grown in slide culture. Normally grown cells (b); Cell morphology by
518 addition of 1 μM pyrogallol (c); by addition of 1 μM pyrogallol and 22 U/ml catalase (d); by addition of
519 22 U/ml catalase (e); by addition of 0.88 μM H_2O_2 (f). (scale bar = 10 μM) (g-i) Box-and-whisker plot
520 of tip-to-branch and branch-to-branch lengths. Effects by pyrogallol (1 μM) (g); Effects of pyrogallol (1
521 μM) with catalase (22 U/ml) (h); Effects of H_2O_2 (0.88 μM) (i). Center lines show the medians; box
522 limits indicate the lower and upper quartile; whiskers extend to 5 and 95 %. Data points are plotted as
523 dots (n=422, 616 sample points).

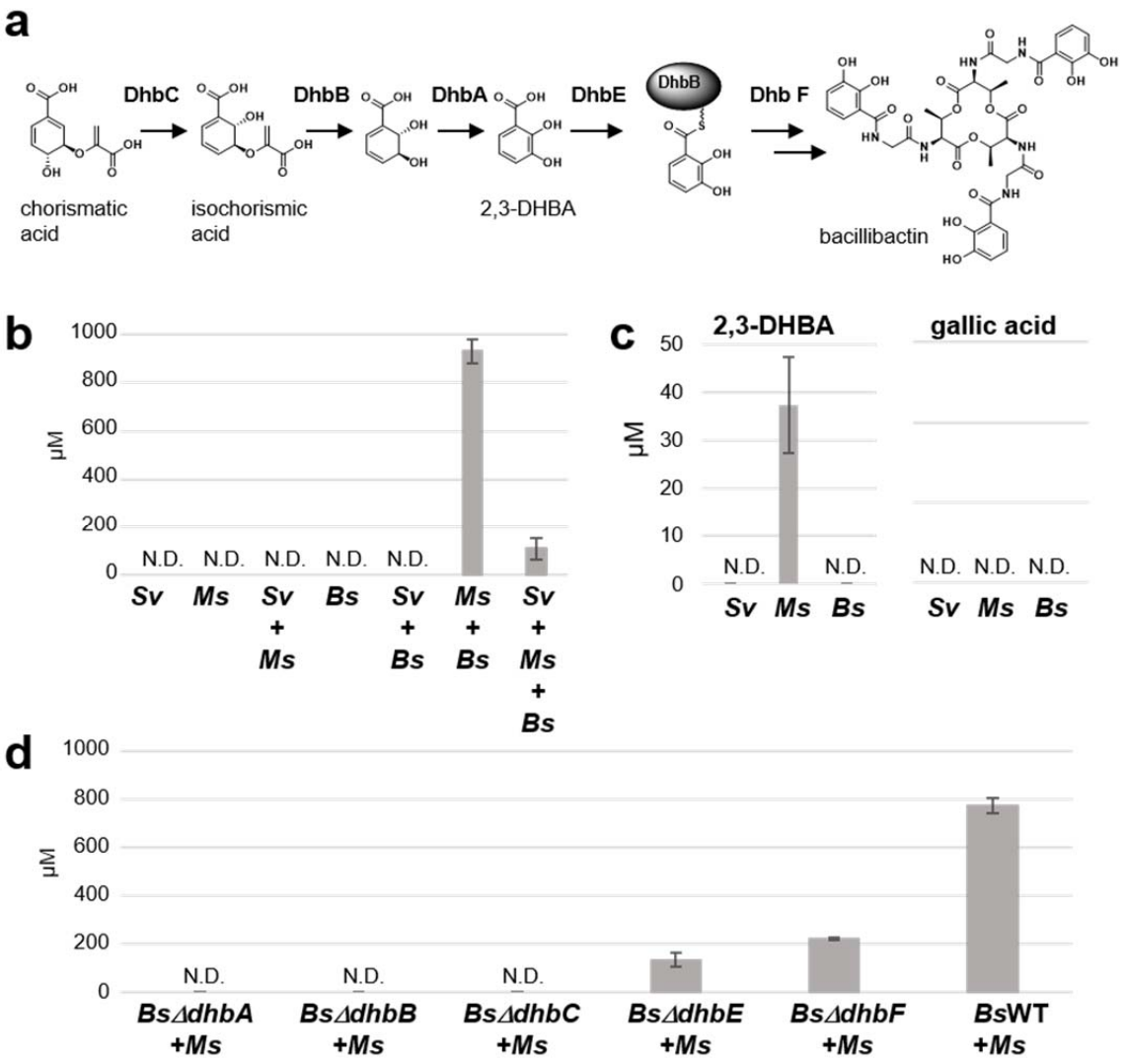

FIG 3 Biosynthetic origin of pyrogallol. (a) Biosynthetic pathway of bacillibactin in *B. subtilis*. (b) Production of pyrogallol in single-, dual- and triple-culture. (c) Feeding of 2,3-DHBA or gallic acid as potential precursor in the culture of Sv, Ms, and Bs. (d) Co-culture of Ms with bacillibactin biosynthetic gene disruptants (Δ*dhbA-F*) of Bs. Sv: *S. variegatus* HEK138A; Ms: *M. septicum* HEK138M; Bs: *B. subtilis* 168. (N.D.: not detected)

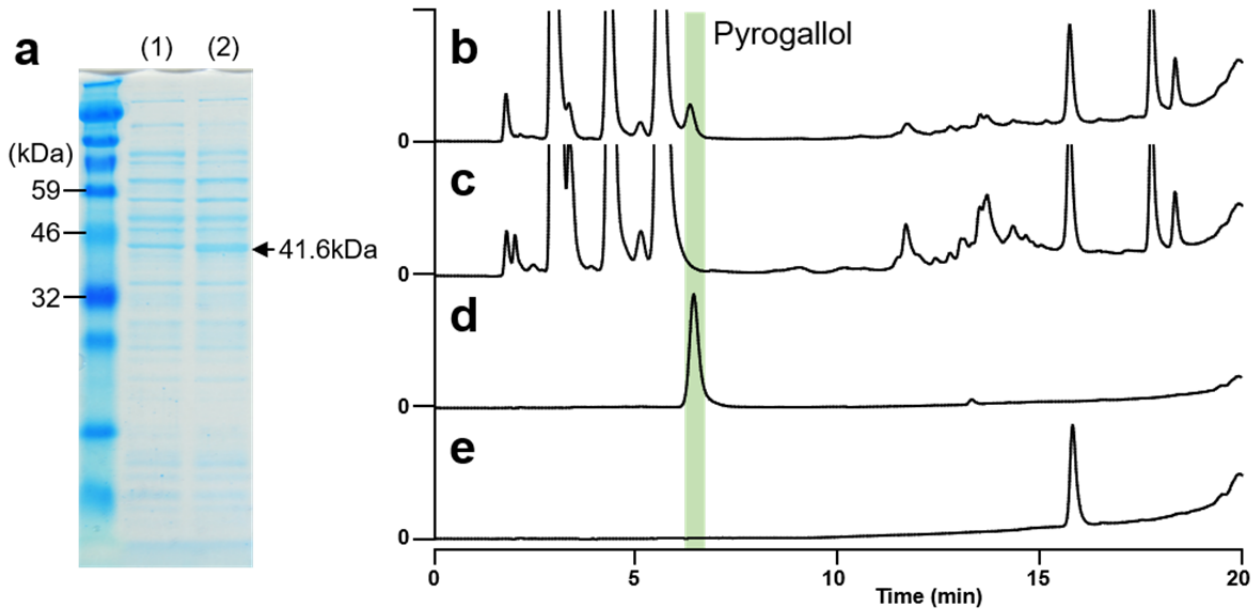

530 **FIG 4** Bioconversion of 2,3-DHBA to pyrogallol by NahG^{Ms}. (a) SDS-PAGE of soluble protein fraction

531 form *E. coli* expressing NahG^{Ms} (2) and negative control with empty vector (1). (b-e) PDA-HPLC traces

532 of bioconversion from 2,3-DHBA to pyrogallol. (b) Incubation of 2,3-DHBA with *E. coli* resting cell

533 expressing NahG^{Ms}. (c) Incubation of 2,3-DHBA with *E. coli* resting cell. (empty vector control) (d)

534 Pyrogallol standard. (e) 2,3-DHBA standard.

535

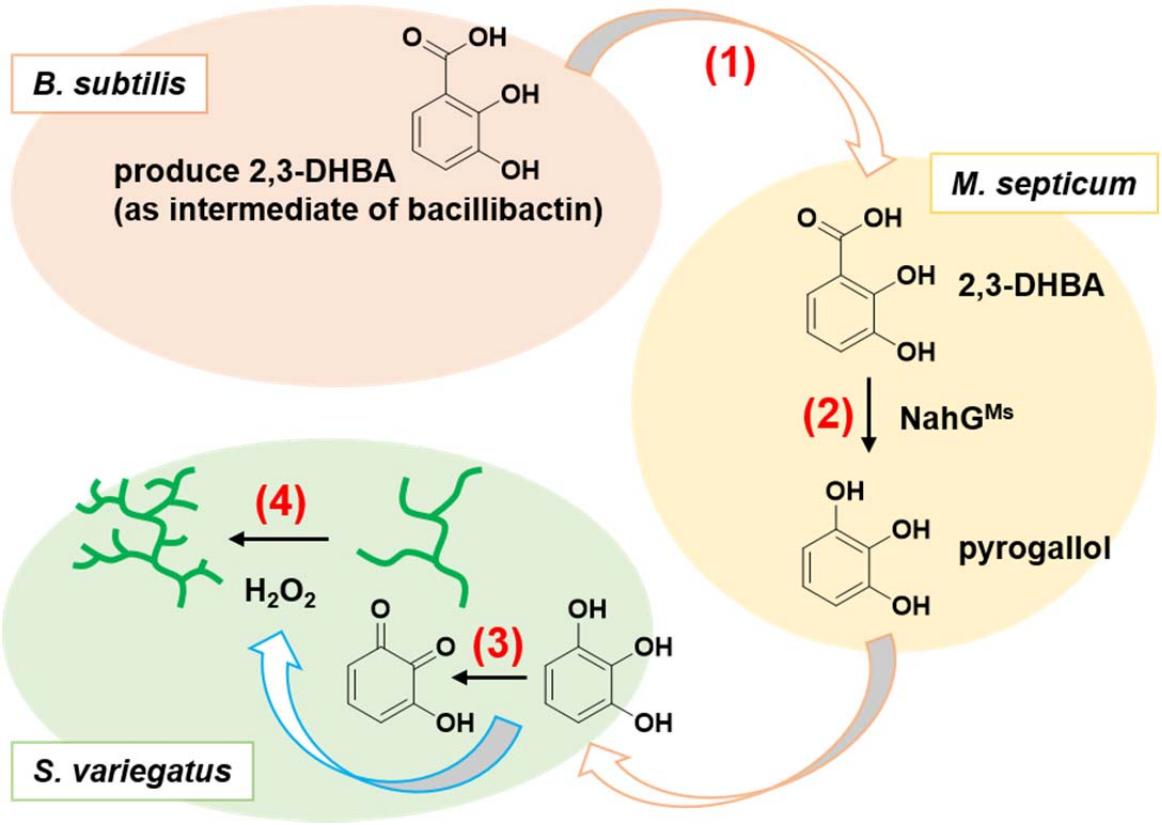

536 **FIG 5** Summary of triple bacterial interaction. (1) *B. subtilis* secrete 2,3-DHBA as intermediate of

537 siderophore bacillibactin. (2) *M. septicum* HEK138M convert 2,3-DHBA to pyrogallol by $NahG^{Ms}$

538 (salicylate 1-monooxygenase). (3) pyrogallol convert to quinone-form and result in generation of H_2O_2.

539 (4) H_2O_2 induce emergence of hyphae branch in *Streptomyces* species.

540